

Combating viral contaminants in CHO cells by engineering STAT1 mediated innate immunity

Austin W.T. Chiang^{1,2}, Shangzhong Li^{2,3}, Benjamin P. Kellman^{1,2,4}, Gouri Chattopadhyay⁵, Yaqin Zhang⁵, Chih-Chung Kuo^{1,2,3}, Jahir M. Gutierrez^{1,2,3}, Faezeh Ghazi¹, Hana Schmeisser⁶, Patrice Ménard⁷, Sara Petersen Bjørn⁷, Bjørn G. Voldborg⁷, Amy S. Rosenberg⁵, Montserrat Puig^{5,+,*} and Nathan E. Lewis^{1,2,3,+,*}

¹ Department of Pediatrics, University of California, San Diego, La Jolla, CA 92093, USA

² The Novo Nordisk Foundation Center for Biosustainability at the University of California, San Diego, La Jolla, CA 92093, USA

³ Department of Bioengineering, University of California, San Diego, La Jolla, CA 92093, USA

⁴ Bioinformatics and Systems Biology Graduate Program, University of California, San Diego, La Jolla, CA 92093, USA

⁵ Center for Drug Evaluation and Research, U.S. Food and Drug Administration, Silver Spring, MD 20993, USA.

⁶ Viral Pathogenesis Section, Laboratory of Immunoregulation, National Institute of Allergy and Infectious Disease, National Institutes of Health, Bethesda, MD 20892, USA

⁷ The Novo Nordisk Foundation Center for Biosustainability, Technical University of Denmark, Hørsholm, Denmark

⁺ These authors contributed equally to this work

^{*} Co-corresponding authors:

Name: Nathan E. Lewis

Address: 9500 Gilman Drive MC 0760, La Jolla, CA 92093

Phone: 858-246-1876

E-mail: nlewisres@ucsd.edu

Name: Montserrat Puig

Address: 10903 New Hampshire Avenue, Silver Spring, MD 20993

Phone: 240-402-7329

E-mail: Montserrat.puig@fda.hhs.gov

Short running title: Virus resistance in CHO cells.

33 Abstract

34 Viral contamination in biopharmaceutical manufacturing can lead to shortages in the supply of critical
 35 therapeutics. To facilitate the protection of bioprocesses, we explored the basis for the susceptibility of
 36 CHO cells, the most commonly used cell line in biomanufacturing, to RNA virus infection. Upon
 37 infection with certain ssRNA and dsRNA viruses, CHO cells fail to generate a significant interferon
 38 (IFN) response. Nonetheless, the downstream machinery for generating IFN responses and its antiviral
 39 activity is intact in these cells: treatment of cells with exogenously-added type I IFN or poly I:C prior to
 40 infection limited the cytopathic effect from Vesicular stomatitis virus (VSV), Encephalomyocarditis
 41 virus (EMCV), and Reovirus-3 virus (Reo-3) in a STAT1-dependent manner. To harness the intrinsic
 42 antiviral mechanism, we used RNA-Seq to identify two upstream repressors of STAT1: Gfi1 and
 43 Trim24. By knocking out these genes, the engineered CHO cells exhibited increased resistance to the
 44 prototype RNA viruses tested. Thus, omics-guided engineering of mammalian cell culture can be
 45 deployed to increase safety in biotherapeutic protein production among many other biomedical
 46 applications.

47

48

49 **Key words:** virus infection, CHO cells, RNA-Seq, anti-viral response, innate immune response, virus
 50 resistance, poly I:C, type I interferon response.

Introduction

Chinese hamster ovary (CHO) cells are extensively used to produce biopharmaceuticals¹ for numerous reasons. Though one advantage is their reduced susceptibility to many human virus families²⁻⁴, there have been episodes of animal viral contamination of biopharmaceutical production runs, mostly from trace levels of viruses in raw materials. These infections have led to expensive decontamination efforts and threatened the supply of critical drugs⁵⁻⁷. Viruses that have halted production of valuable therapeutics include RNA viruses such as Cache Valley virus⁶, Epizootic hemorrhagic disease virus⁸, Reovirus⁶ and Vesivirus 2117⁹. Thus, there is a critical need to understand the mechanisms by which CHO cells are infected and how the cells can be universally engineered to enhance their viral resistance¹⁰. For example, a strategy was proposed to inhibit infection of CHO cells by minute virus of mice by engineering glycosylation¹¹. We present an alternative strategy to prevent infections of a number of RNA viruses with different genomic structures and strategies to interfere with the host anti-viral defense.

Many studies have investigated the cellular response to diverse viruses in mammalian cells, and detailed the innate immune responses that are activated upon infection. For example, type I interferon (IFN) responses play an essential role in regulating the innate immune response and inhibiting viral infection¹²⁻¹⁵ and can be induced by treatment of cells with poly I:C¹⁶⁻¹⁸. However, the detailed mechanisms of virus infection and the antiviral response in CHO cells remain largely unknown. Understanding the role of type I IFN-mediated innate immune responses in CHO cells could be invaluable for developing effective virus-resistant CHO bioprocesses. Fortunately, the application of recent genome sequencing¹⁹⁻²³ and RNA-Seq tools can now allow the analysis of complicated cellular processes in CHO cells²⁴⁻²⁸, such as virus infection.

To unravel the response of CHO cells to viral infection, we infected CHO-K1 cells with RNA viruses from diverse virus families. We have further assayed the ability of activators of type I IFN pathways to induce an antiviral response in the cells. Specifically, we asked the following questions: (1)

Can CHO-K1 cells mount a robust type I IFN response when infected by RNA viruses? (2) Can innate immune modulators trigger a type I IFN response of CHO-K1 cells and, if so, are the type I IFN levels produced sufficient to protect CHO-K1 cells from RNA virus infections? (3) Which biological pathways and processes are activated during virus infection and/or treatment with innate immune modulators, and are there common upstream regulators that govern the antiviral response? (4) Upon the identification of common upstream regulators, how can we engineer virus resistance into CHO cells for mitigating risk in mammalian bioprocessing? Here we address these questions, illuminate antiviral mechanisms of CHO cells, and guide the development of bioprocess treatments and cell engineering efforts to make CHO cells more resistant to viral infection.

Materials and Methods

CHO-K1 cells and RNA virus infections

The susceptibility of CHO-K1 cells to viral infection has been previously reported³. Since infectivity was demonstrated for viruses of a variety of families (harboring distinct genomic structures), we selected the following RNA viruses from three different families to be used as prototypes: Vesicular stomatitis virus (VSV, ATCC® VR-1238), Encephalomyocarditis virus (EMCV, ATCC® VR-129B), and Reovirus-3 virus (Reo-3, ATCC® VR-824). Viral stocks were generated in susceptible Vero cells as per standard practices using DMEM (Dulbecco's Modified Eagle's medium) supplemented with 10% FBS, 2mM L-glutamine, 100 U/ml penicillin and 100 µg/ml streptomycin (DMEM-10). Viral stocks were titered by tissue culture infectious dose 50 (TCID₅₀) on CHO-K1 cells and used to calculate the multiplicity of infection in the experiments (Table 1).

Virus infection procedures. Cells were seeded in cell culture plates (3x10⁵ and 1.2x10⁶ cells/well in 96-well and 6-well plates, respectively) and grown overnight in RPMI-1040 supplemented with 10%

100 FBS, 2mM L-glutamine, 100 U/ml penicillin and 100 µg/ml streptomycin, 10 mM Hepes, 1x non-
 101 essential amino acids and 1 mM sodium pyruvate (RPMI-10). IFNα/β (human IFNα (Roferon) and IFNβ
 102 (Avonex), mouse IFNα (Bei Resources, Manassas, VA)) as well as innate immune modulators (LPS
 103 (TLR4) (Calbiochem), CpG-oligodeoxynucleotide (ODN) D-ODN, 5'-
 104 GGTGCATCGATGCAGGGGG-3'²⁹ and ODN-1555, 5'-GCTAGACGTTAGCGT-3' (TLR9) (custom-
 105 synthesized at the Center for Biologics Evaluation and Research facility, FDA), imidazoquinoline R837
 106 (TLR7/8) (Sigma) and poly I:C-Low molecular weight/LyoVec (poly I:C) (Invivogen) were added to
 107 the cultures 24 h prior to testing or virus infection, at the concentrations indicated in the figures. Note
 108 that, by monitoring changes in the gene expression levels of IFNβ and Mx1 in the cells, we established
 109 that 16-20 h would be an adequate time interval for treating cells with poly I:C prior to infection (Figure
 110 S1). Anti-IFNβ neutralizing antibody (2.5 µg/ml; Abcam, Cambridge, MA cat# 186669) was also used
 111 in certain experiments, 24 h prior to infection. Viral infection was performed by adding virus suspensions
 112 to the cell monolayers at the indicated MOI in serum-free media and incubated at 37 °C, 5% CO₂ for 2h.
 113 Cell cultures were washed twice to discard unbound virus and further incubated at 37 °C for 30 h (VSV),
 114 54 h (EMCV) or 78 h (Reo-3) (unless otherwise indicated in the figures). The cell harvesting time was
 115 established based on appearance of cytopathic effect in approximately 50% of the cell monolayer.
 116 Cytopathic effect was visualized by crystal violet staining as per standard practices. Infection/poly I:C
 117 experiments were repeated twice, independently. In each experiment, CHO cells were cultured as poly
 118 I:C untreated – uninfected (media control, m), poly I:C treated – uninfected (p), poly I:C untreated –
 119 virus infected (Vm) and poly I:C treated – virus infected (Vp).

120 **Western blot procedures.** Cell lysates were prepared using mammalian protein extraction reagent
 121 M-PER (Thermo Fisher Scientific, Waltham, MA) with Protease and Halt™ phosphatase inhibitor
 122 cocktails (Thermo Fisher Scientific) using an equal number of cells per sample. Samples were analyzed
 123 by SDS-PAGE using 10-20% Tris-Glycine gels (Thermo Fisher Scientific) under reducing conditions.

As a molecular weight marker, protein ladder (cat# 7727S) from Cell Signaling Technology (Danvers, MA) was used. Nitrocellulose membranes and iBlot™ transfer system (Thermo Fisher Scientific) were used for Western Blot analysis. All other reagents for Western Blot analyses were purchased from Thermo Fisher Scientific. Membranes were blocked with nonfat dry milk (BIO-RAD, Hercules, CA) for 1h followed by incubation with primary antibodies against STAT1, pSTAT1 (pY701, BD Transduction Lab, San Jose, CA), pSTAT2 (pY689, Millipore Sigma, Burlington, MA), actin (Santa Cruz Biotechnology, Santa Cruz, CA) or Mx1 (gift from O. Haller, University of Freiburg, Freiburg, Germany) O/N at 4°C. Secondary goat anti-mouse and anti-rabbit antibodies were purchased from Santa Cruz Biotechnology. SuperSignal West Femto Maximum Sensitivity Kit (Thermo Fisher Scientific) was used to develop membranes, and images were taken using LAS-3000 Imaging system (GE Healthcare Bio-Sciences, Pittsburgh, PA).

RNA extraction, purification, and real-time PCR

Cell cultures were re-suspended in RLT buffer (Qiagen) and kept at -80°C until RNA was extracted using the RNeasy kit (Qiagen) and on-column DNase digestion. RNA was eluted in 25 µl of DEPC water (RNase/DNase free); concentration and purity were tested by bioanalyzer. Total RNA levels for type I IFN related genes and viral genome were also assessed by RT-PCR. Complementary DNA synthesis was obtained from 1 µg of RNA using the High capacity cDNA RT kit (Thermo Fisher scientific) as per manufacturer's instructions. Semi-quantitative PCR reactions (25 µl) consisted in 1/20 cDNA reaction volume, 1x Power Sybr master mix (Thermo Fisher Scientific), 0.5 µM Chinese hamster-specific primers for IFNβ, Mx1, IRF7 and IITMP3 sequences (SABiosciences). Eukaryotic 18S was used as a housekeeping gene and assessed in 1X Universal master mix, 18S expression assay (1:20) (Applied Biosystems) using a 1/50 cDNA reaction volume. Fold changes were calculated by the 2-ΔΔCt method.

cDNA library construction and Next-generation sequencing (RNA-Seq)

Library preparation was performed with Illumina's TruSeq Stranded mRNA Library Prep Kit High Throughput (Catalog ID: RS-122-2103), according to manufacturer's protocol. Final RNA libraries were first quantified by Qubit HS and then QC on Fragment Analyzer (from Advanced Analytical). Final pool of libraries was run on the NextSeq platform with high output flow cell configuration (NextSeq® 500/550 High Output Kit v2 (300 cycles) FC-404-2004). Raw data are deposited at the Gene Expression Omnibus and Short Read Archive (accession numbers: GSE119379)

RNA-Seq quantification and differential gene expression analysis

RNA-Seq quality was assessed using FastQC. Adapter sequences and low-quality bases were trimmed using Trimmomatic³⁰. Sequence alignment was accomplished using STAR³¹ against the CHO genome (GCF_000419365.1_C_griseus_v1.0) with default parameters. HTSeq³² was used to quantify the expression of each gene. We performed differential gene expression analysis using DESeq2³³. After Benjamini-Hochberg FDR correction, genes with adjusted p-values less than 0.05 and fold change greater than 1.5 were considered as differentially expressed genes (DEGs). Table S1 shows the number of identified DEGs in the three different comparisons: 1) untreated – uninfected vs. untreated – virus infected (m vs. Vm); 2) untreated – uninfected vs. poly I:C treated – uninfected (m vs. p); and 3) untreated – virus infected vs. poly I:C treated – virus infected (Vm vs. Vp).

Genetic engineering (Gfi1, Trim24, Gfi1/Trim24) of CHO-S cell lines

CHO-S cells (Thermo Fisher Scientific Cat. # A1155701) and KO clones were cultured in CD CHO medium supplemented with 8 mM L-glutamine and 2 mL/L of anti-clumping agent (CHO medium) in an incubator at 37°C, 5% CO₂, 95% humidity. Cells were transfected using FuGENE HD reagent (Promega Cat. # E2311). The day prior to transfection, viable cell density was adjusted to 8×10^5 cells/mL in an MD6 plate well containing 3 mL CD CHO medium supplemented with 8 mM L-glutamine. For

each transfection, 1500 ng Cas9-2A-GFP plasmid and 1500 ng gRNA plasmid (see Text S1 for details about the construction of plasmids) were diluted in 75 μ L OptiPro SFM. Separately, 9 μ L FuGene HD reagent was diluted in 66 μ L OptiPro SFM. The diluted plasmid was added to the diluted FuGENE HD and incubated at room temperature for 5 minutes and the resultant 150 μ L DNA/lipid mixture was added dropwise to the cells. For viability experiments, CHO-S KO cell lines were seeded at 3×10^6 cells in 30 ml in CHO medium and incubated at 37 °C, 5% CO₂, 125 rpm for up to 7 days. Infections were conducted with EMCV and Reo-3 at the same MOI calculated in CHO-K1 cells for 2h prior to wash cells twice to discard unbound particles. Control cell lines showing susceptibility to either virus were infected in parallel to those with Gfi1 and Trim24 gene KO.

Results and Discussion

CHO-K1 cells fail to resolve infection by RNA viruses despite possessing functional type I IFN-inducible anti-viral mechanisms

To evaluate the response of CHO cells to three different RNA viruses (VSV, EMCV and Reo-3; see Table 1), cells were infected and monitored for cytopathic effects and gene expression changes related to the type I IFN response. All three viruses induced a cytopathic effect (Figure 1A, right panels) and a modest increase in IFN β transcript levels in infected CHO cell cultures was measured (Figure 1B), suggesting limited production of IFN. Through its cellular receptor, IFN α/β can further activate downstream interferon-stimulated genes known to limit viral infection both in cell culture and *in vivo*³⁴⁻³⁷. We noted that CHO cells seem to have a functional IFN α/β receptor and its activation with exogenous IFN confers resistance of CHO cells to VSV infection (see Supplementary Information Text S2 and Figure S2). Interestingly, CHO cells expressed high levels of the antiviral gene Mx1 when infected with Reo-3, but not VSV and EMCV (Figure 1C). Nevertheless, the virus-induced IFN mRNA response in

the host cell was insufficient to prevent cell culture destruction. These data suggest a possible inhibition of the antiviral type I IFN response that varies across viruses, as previously reported³⁸⁻⁴¹.

To explore why the induced type I IFN failed to mount a productive antiviral response in CHO cells, we conducted RNA-Seq and pathway analysis using GSEA (see details in Text S3 and Table S1). GSEA analysis that compared control vs. infected CHO cells (m vs. Vm) revealed the modulation of several immune-related gene sets and pathways activated by the virus (Figures 1D and S3, Table S2, and Text S4). Unlike VSV and EMCV, Reo-3 induced the ‘interferon alpha response’ and ‘RIG-I and MDA5-mediated induction of IFN α ’ pathways ((p-value, NES) = (9.05x10⁻³, 3.68) and (1.12x10⁻², 2.74), respectively). These findings were consistent with observations that the reovirus genome (dsRNA) can stimulate TLR3 and RIG-I to induce innate immune responses in other cell types⁴²⁻⁴⁴, in which the observed responses diverged markedly from the VSV and EMCV infections.

As we observed for Mx1, only Reo-3-infected cells showed a significant enrichment of differentially expressed genes involved in the type I IFN response (FDR-adjusted p-value = 9.05x10⁻³; normalized enrichment score, NES = 3.68). These genes contain the consensus transcription factor binding sites in the promoters that are mainly regulated by the transcription factor STAT1 and the interferon regulatory factors (IRF) family, such as IRF1, IRF3, IRF7 and IRF8 (Figure 1E). These results are consistent with observations that the IRF family transcription factors activate downstream immune responses in virus-infected mammalian cells^{45, 46}. In contrast, VSV and EMCV failed to trigger anti-viral related mechanisms (e.g., type I IFN responses) downstream of IFN β (Figures 1D and S3A). Examples of a few pathways that were stimulated included ‘immune system’ (including adaptive/innate immune system and cytokine signaling in immune system) in VSV (FDR-adjusted p-value = 1.49x10⁻²; normalized enrichment score, NES= 1.99) and the ‘G2M checkpoint’ in EMCV (p-value = 8.95x10⁻³; NES = 2.64). Disruption of the cell cycle affecting the G2M DNA checkpoint network has been reported for the survival of several viruses, including HIV (ssRNA)⁴⁷, EBV (dsDNA)⁴⁸, JCV (DNA)⁴⁹, HSV (DNA)⁵⁰. However, further studies will need to confirm whether VSV or EMCV use a similar strategy

to escape the cell defense. Nevertheless, neither VSV nor EMCV infection activated known upstream activators of type I IFN pathways (Figure 1E) when analyzed with Ingenuity Pathway Analysis (IPA)⁵¹.

Poly I:C induces a robust type I interferon response in CHO cells

Type I IFN responses limit viral infection¹²⁻¹⁵, and innate immune modulators⁵²⁻⁵⁴ mimic pathogenic signals and stimulate pattern recognition receptors (PRRs), leading to the activation of downstream immune-related pathways. Intracellular PRRs, including toll-like receptors (TLR) 7, 8 and 9, and cytosolic receptors RIG-I or MDA5, can sense viral nucleic acids and trigger the production of type I IFN. Thus, we asked whether CHO cell viral resistance could be improved by innate immune modulators.

CHO PRRs have not been studied extensively, so we first assessed the ability of synthetic ligands to stimulate their cognate receptors to induce a type I IFN response. CHO cells were incubated with LPS (TLR4 ligand), CpG-oligodeoxynucleotide (ODN) type D (activates TLR9 on human cells), ODN-1555 (activates TLR9 on murine cells), imidazoquinoline R837 (TLR7/8 ligand) and poly I:C-Low molecular weight/LyoVec (poly I:C) (activates the RIG-I/MDA-5 pathway), and subsequently tested for changes in expression of IFN stimulated genes with anti-viral properties. After 24 h of culture, gene expression levels of IRF7 and Mx1 increased significantly in cells treated with poly I:C but not in those treated with any of the other innate immune modulators (Figure 2A). Furthermore, STAT1 and STAT2 phosphorylation and Mx1 protein levels were elevated following treatment with poly I:C or exogenous interferon-alpha (IFN α), which was used as a control (Figure 2B and 2C).

Next, we characterized the type I IFN response induced by poly I:C by analyzing the transcriptome of untreated vs. treated CHO cells. Cells were cultured with poly I:C in the media for 30, 54 and 78 h after an initial 16 h pre-incubation period (see Methods for details). GSEA of the RNA-Seq data demonstrated that poly I:C induced a strong ‘innate immune response’ in comparison to untreated cultures (media) (m vs. p; (p-value, NES, Enrichment strength) = (8.08x10⁻³, 2.98, 73%), (1.57x10⁻², 3.95, 70%) and (3.91x10⁻³, 3.58, 78%)) evident in the three independently tested time points (Figures

2D and S3B, Text S4 and Table S3). In addition, poly I:C activated several upstream regulators of the type I IFN pathways (Figure 2E). We note that the GSEA strength (see Text S3) of the innate immune response induced by poly I:C (m vs. p) was stronger than the innate immune response seen for Reo-3 infection alone (m vs. Vm in Figure S3). Thus, CHO cells can activate the type I IFN signaling (JAK-STAT) pathway in response to poly I:C and display an anti-viral gene signature, which was sustained for at least 4 days.

Poly I:C-induced type I interferon response protects CHO cells from RNA virus infections

We next examined if the type I IFN response, induced by poly I:C, could protect CHO cells from RNA virus infections. We found that poly I:C pre-treatment protected CHO cells against VSV infection through the IFN β -mediated pathway (Figure S4 and Text S5), and that poly I:C protected against all three viruses tested (Figures 3A-C). Cell morphology differed notably between cultures infected with virus (Vm), control uninfected cells (m), and poly I:C pre-treated cultures (p and Vp) (Figures 3A-C, left panels). These morphological changes correlated with the cytopathic effect observed in the cell monolayers (Figures 3A-C, right panels). At 78h, the extent of cell culture damage by Reo-3, however, was milder than by VSV and EMCV at a shorter incubation times (30h and 54h, respectively) (Panels Vm in Figures 3A-C), possibly since Reo-3 induced higher levels of anti-viral related genes in the CHO cells but VSV and EMCV did not (Figures 1C, 1D and 1E). Notably, although poly I:C pre-treatment conferred protection of CHO cells to all three viral infections (Panels Vp in the Figure 3A-C), striking transcriptomic differences were observed (Table S4). Poly I:C pre-treatment significantly activated immune-related pathways and up-regulated type I IFN-related gene expression in CHO cells infected with VSV and EMCV when compared to non-poly I:C pre-treated cells that were infected (Vm vs. Vp) (Figures 3D-E, S5A-B and Table S5). Poly I:C pre-treatment was sufficient to induce a protective type I IFN response to VSV and EMCV. In contrast, for Reo-3 infection, pre-treatment with poly I:C did not

272 further increase the levels of expression of IFN associated genes already observed in no pre-treated cells.
 273 The lack of enhanced expression of antiviral genes in Reo-3 Vm vs. Vp observed in the GSEA was
 274 further confirmed by Taqman analysis. A similar level of expression of anti-viral Mx1 and IITMP3
 275 genes⁵⁵⁻⁵⁸ was obtained for CHO cells independently infected with Reo-3 (Vm), treated with poly I:C
 276 (p), or pre-treated with poly I:C and infected (Vp), which resulted in no differences in transcript levels
 277 when we compared Vm vs. Vp (Figure S5C). Nevertheless, the outcome of infection was surprisingly
 278 different in Vm or Vp samples. To understand these differences, we searched for genes that were
 279 differently modulated by poly I:C treatment in the context of Reo-3 infection. Indeed, we identified 30
 280 genes (Figure S6 and Table S6) that were significantly up regulated (adjusted p-value <0.05, fold change
 281 >1.5) in the comparisons of m vs. Vp and m vs. p but not in the comparison of m vs. Vm. These genes
 282 are significantly enriched in 11 KEGG pathways related to host-immune response (e.g., antigen
 283 processing and presentation, p-value=3.4x10⁻³) and processes important to virus infection (e.g.,
 284 endocytosis, p-value=2.5x10⁻²). We also observed many of these genes significantly enriched molecular
 285 functions: 1) RNA polymerase II transcription factor activity (11 genes; GO:0000981 FDR-adjusted p-
 286 value < 1.30x10⁻¹⁵) and 2) nucleic acid binding transcription factor activity (12 genes GO:0001071 FDR-
 287 adjusted p-value < 3.54x10⁻¹⁵) by gene set enrichment analysis (see Text S3 and Table S7). This suggests
 288 that poly I:C treatment, 16 hours prior to virus infection, pre-disposes the cell to adopt an antiviral state
 289 and might restore the host transcription machinery subverted by Reo-3 virus resulting in the protection
 290 of the CHO cells.

291 Our results revealed other processes that are differentially activated or repressed between Vm
 292 and Vp (Figure 3D and Table S4). For example, the top down-regulated Reactome pathways in the virus-
 293 infected cells (Vm vs. Vp) are protein translational related processes: ‘nonsense mediated decay
 294 enhanced by the exon junction complex’ (p-value = 3.32x10⁻², NES = -3.50), ‘peptide chain elongation’
 295 (p-value = 3.32x10⁻², NES = -3.59), and ‘3’-UTR mediated translational regulation’ (p-value = 3.38x10⁻², NES = -3.61). These results agree with studies showing viral hijacking of the host protein translation

297 machinery during infection⁵⁹, and that the activation of interferon-stimulated genes restrain virus
 298 infections by inhibiting viral transcription and/or translation¹². All these results suggest that poly I:C
 299 treatment provides the cell with an advantageous immune state that counteracts viral escape mechanisms
 300 and results in cell survival.

301 302 **A STAT1-dependent regulatory network governs viral resistance in CHO cells**

303 GSEA revealed that several transcriptional regulators were activated or repressed during different viral
 304 infections and poly I:C-treated cells (Figures 1E, 2E, and 3E). Among these, NFATC2, STAT1, IRF3,
 305 IRF5, and IRF7 were consistently activated by poly I:C pre-treatment of CHO cells (m vs. p and Vm vs.
 306 Vp), and TRIM24 was suppressed. These transcription factors are involved in TLR-signaling (IRF3,
 307 IRF5, and IRF7)⁴⁵ and JAK/STAT signaling (NFATC2, STAT1, and TRIM24). The TLR signaling
 308 pathway is a downstream mediator in virus recognition/response and in activating downstream type-I
 309 interferon immune responses⁶⁰⁻⁶². Meanwhile, the JAK/STAT pathway contributes to the antiviral
 310 responses by up-regulating interferon stimulated genes to rapidly eliminate virus within infected cells⁶³⁻
 311 ⁶⁵. Importantly, one mechanism by which STAT1 expression and activity may be enhanced is via the
 312 poly I:C-induced repression of TRIM24 (an inhibitor of STAT1). The crosstalk between TLR- and
 313 JAK/STAT-signaling pathways is therefore important in virus clearance of infected host cells⁶⁶.

314 In order to better understand the role of upstream regulators in the CHO cell viral protection, we
 315 examined the expression of the affected downstream target genes. Table 2 shows the regulatory pathways
 316 modulated by poly I:C treatment in uninfected (m vs. p; Table 2A) or infected (Vm vs. Vp; Table 2B)
 317 cells, and the described downstream effect. In cells surviving VSV and EMCV infection (Vp), we
 318 identified regulatory networks involved in restricting viral replication (Table 2B and Figures 4A and
 319 4B). These networks are predominantly regulated by the 6 transcription factors (NFATC2, STAT1,
 320 IRF3, IRF5, IRF7, and TRIM24) that were also identified as transcription factors induced in poly I:C
 321 treated uninfected cells (p) (Table 2A). These findings suggest that the induction of the STAT1-

dependent regulatory network by poly I:C treatment allows the cell to adopt an activated state that makes it refractory to virus infection. In contrast, the STAT1-dependent regulatory network was not apparent when comparing Reo-3 infected cells untreated and treated with poly I:C (Vm vs. Vp), because both Reo-3 and poly I:C induce STAT1 in CHO cells (Figure 1E and 2E). Poly I:C is a structural analog of double-stranded RNA and activates similar pathways as Reo-3⁶⁷, such as, the NFATC2-dependent (Figures S7) and IRF3-dependent networks (Figures S8).

With the STAT1 network potentially contributing to viral resistance, we searched for upstream regulators that could be modulated to maximally induce STAT1. We identified sixteen statistically significant ($p < 0.05$) upstream regulators, including 13 positive and 3 negative regulators of STAT1 using IPA (Figure 5; see details in Text S6). We hypothesized that the deletion of the most active repressors of STAT1 could improve virus resistance by inducing STAT1 gene expression and the downstream type I IFN antiviral response in the cell (Figure 5). We identified three STAT1 repressors (Trim24, Gfi1 and Cbl) with a negative regulatory score and therefore potential for inhibiting STAT1 based on the RNA-Seq differential expression data (see details in Text S6 and Figure S9). However, Cbl was not present in cells infected with Reo-3 (Table S8). Therefore, we selected the two negative regulators, Gfi1⁶⁸ and Trim24⁶⁹ of STAT1 as knockout targets for genetic engineering in CHO-S cells and subsequently tested the virus susceptibility of such KO cells, using Reo-3 and EMCV. We found that the Trim24 and Gfi1 single knockout clones showed resistance to Reo-3 but moderate or no resistance against EMCV (Figure 6A-B), compared to virus susceptible positive control cell lines (Figure S10). However, the Gfi1 + Trim24 double knockout (Figure 6C) showed resistance to both viruses tested, even when cells were passaged and cultured for an additional week (Figure S11). Together these results show that eliminating repressors of the STAT1 regulatory network contributes to antiviral mechanisms of CHO cells, which could possibly be harnessed to obtain virus-resistant CHO bioprocesses.

Conclusions

Here we perform a genome-wide study of viral resistance in CHO, thereby demonstrating the utility of systems biology approaches to not only improve host cell productivity and metabolism⁷⁰⁻⁷², but also to improve product safety. Specifically, we demonstrated that STAT1 and other key regulators contribute to the inhibition of RNA virus replication in CHO cell lines. Furthermore, an analysis of poly I:C treatment exposed these molecular mechanisms underlie the protection against RNA virus infection. Studies have shown that modulating genetic factors can promote viral resistance in CHO cells^{11, 73, 74}. However, our findings suggest novel cell engineering targets beyond those coding for cell receptors. Thus, these insights provide further tools to enable the development of virus-resistant hosts to improve safety and secure the availability of biotherapeutic products^{3, 75, 76}.

Acknowledgments

This work was supported by generous funding from the Novo Nordisk Foundation provided to the Center for Biosustainability at the Technical University of Denmark (grant no. NNF10CC1016517). Funding was also received from the Regulatory Science and Review Enhancement program at the FDA (RSR #14-07).

Author contributions

ASR conceived of the project idea; MP, ASR, NEL directed the research; AWTC, MP, and NEL wrote the manuscript; AWTC, SL, BPK, CCK, JMG, and FG analyzed the RNA-Seq data; PM, SPB, BGV conducted the RNA-Seq; MP, GC, YZ and HS conducted CHO cell and virus experiments. All authors read and approved of this work.

Reference

1. Walsh, G. Biopharmaceutical benchmarks 2014. *Nat Biotechnol* **32**, 992-1000 (2014).
2. Weiebe, M.E. et al. A multifaceted approach to assure that recombinant tPA is free of adventitious virus. In: Advances in animal cell biology and technology for bioprocesses. (Spier, Griffiths, Stephenne, Crooy, eds.). 68-71 (1989).
3. Berting, A., Farcet, M.R. & Kreil, T.R. Virus susceptibility of Chinese hamster ovary (CHO) cells and detection of viral contaminations by adventitious agent testing. *Biotechnol Bioeng* **106**, 598-607 (2010).
4. Poiley, J.A., Nelson, R.E., Hillesund, T. & Rainer, i.R. Susceptibility of cho k1 cells to infection by eight adventitious viruses and four retroviruses. *In Vitro Toxicology* **4**, 1-12 (1991).
5. Garnick, R.L. Raw materials as a source of contamination in large-scale cell culture. *Dev Biol Stand* **93**, 21-29 (1998).
6. Nims, R.W. Detection of adventitious viruses in biologicals--a rare occurrence. *Dev Biol (Basel)* **123**, 153-164; discussion 183-197 (2006).
7. Dinowitz, M. et al. Recent studies on retrovirus-like particles in Chinese hamster ovary cells. *Dev Biol Stand* **76**, 201-207 (1992).
8. Rabenau, H. et al. Contamination of genetically engineered CHO-cells by epizootic haemorrhagic disease virus (EHDV). *Biologicals* **21**, 207-214 (1993).
9. Bethencourt, V. Virus stalls Genzyme plant. *Nature Biotechnology* **27**, 681 (2009).
10. Merten, O.W. Virus contaminations of cell cultures - A biotechnological view. *Cytotechnology* **39**, 91-116 (2002).
11. Mascarenhas, J.X. et al. Genetic engineering of CHO cells for viral resistance to minute virus of mice. *Biotechnol Bioeng* **114**, 576-588 (2017).
12. Schoggins, J.W. & Rice, C.M. Interferon-stimulated genes and their antiviral effector functions. *Curr Opin Virol* **1**, 519-525 (2011).
13. Sadler, A.J. & Williams, B.R. Interferon-inducible antiviral effectors. *Nat Rev Immunol* **8**, 559-568 (2008).
14. Perry, A.K., Chen, G., Zheng, D., Tang, H. & Cheng, G. The host type I interferon response to viral and bacterial infections. *Cell Res* **15**, 407-422 (2005).
15. Taniguchi, T. & Takaoka, A. The interferon-alpha/beta system in antiviral responses: a multimodal machinery of gene regulation by the IRF family of transcription factors. *Curr Opin Immunol* **14**, 111-116 (2002).

- 402 16. Pantelic, L., Sivakumaran, H. & Urosevic, N. Differential induction of antiviral effects against
403 West Nile virus in primary mouse macrophages derived from flavivirus-susceptible and congenic
404 resistant mice by alpha/beta interferon and poly(I-C). *J Virol* **79**, 1753-1764 (2005).
- 405 17. Green, T.J. & Montagnani, C. Poly I:C induces a protective antiviral immune response in the
406 Pacific oyster (*Crassostrea gigas*) against subsequent challenge with Ostreid herpesvirus (OsHV-
407 1 muvar). *Fish Shellfish Immunol* **35**, 382-388 (2013).
- 408 18. Plant, K.P., Harbottle, H. & Thune, R.L. Poly I:C induces an antiviral state against Ictalurid
409 Herpesvirus 1 and Mx1 transcription in the channel catfish (*Ictalurus punctatus*). *Dev Comp*
410 *Immunol* **29**, 627-635 (2005).
- 411 19. Lewis, N.E. et al. Genomic landscapes of Chinese hamster ovary cell lines as revealed by the
412 *Cricetulus griseus* draft genome. *Nature Biotechnology* **31**, 759-+ (2013).
- 413 20. Xu, X. et al. The genomic sequence of the Chinese hamster ovary (CHO)-K1 cell line. *Nat*
414 *Biotechnol* **29**, 735-741 (2011).
- 415 21. Vishwanathan, N. et al. Augmenting Chinese hamster genome assembly by identifying regions
416 of high confidence. *Biotechnol J* **11**, 1151-1157 (2016).
- 417 22. Chen, C., Le, H. & Goudar, C.T. Evaluation of two public genome references for Chinese
418 hamster ovary cells in the context of RNA-seq based gene expression analysis. *Biotechnol Bioeng*
419 (2017).
- 420 23. van Wijk, X.M. et al. Whole-Genome Sequencing of Invasion-Resistant Cells Identifies Laminin
421 alpha2 as a Host Factor for Bacterial Invasion. *MBio* **8** (2017).
- 422 24. Wang, Z., Gerstein, M. & Snyder, M. RNA-Seq: a revolutionary tool for transcriptomics. *Nat*
423 *Rev Genet* **10**, 57-63 (2009).
- 424 25. Vishwanathan, N. et al. Global Insights Into the Chinese Hamster and CHO Cell Transcriptomes.
425 *Biotechnology and Bioengineering* **112**, 965-976 (2015).
- 426 26. Yuk, I.H. et al. Effects of copper on CHO cells: insights from gene expression analyses.
427 *Biotechnol Prog* **30**, 429-442 (2014).
- 428 27. Fomina-Yadlin, D. et al. Transcriptome analysis of a CHO cell line expressing a recombinant
429 therapeutic protein treated with inducers of protein expression. *J Biotechnol* **212**, 106-115 (2015).
- 430 28. Hsu, H.H. et al. A Systematic Approach to Time-series Metabolite Profiling and RNA-seq
431 Analysis of Chinese Hamster Ovary Cell Culture. *Sci Rep* **7**, 43518 (2017).
- 432 29. Puig, M. et al. TLR9 and TLR7 agonists mediate distinct type I IFN responses in humans and
433 nonhuman primates in vitro and in vivo. *J Leukocyte Biol* **91**, 147-158 (2012).
- 434 30. Bolger, A.M., Lohse, M. & Usadel, B. Trimmomatic: a flexible trimmer for Illumina sequence
435 data. *Bioinformatics* **30**, 2114-2120 (2014).
- 436 31. Dobin, A. et al. STAR: ultrafast universal RNA-seq aligner. *Bioinformatics* **29**, 15-21 (2013).

- 437 32. Anders, S., Pyl, P.T. & Huber, W. HTSeq--a Python framework to work with high-throughput
438 sequencing data. *Bioinformatics* **31**, 166-169 (2015).
- 439 33. Anders, S. & Huber, W. Differential expression analysis for sequence count data. *Genome Biol*
440 **11**, R106 (2010).
- 441 34. Katze, M.G., He, Y. & Gale, M., Jr. Viruses and interferon: a fight for supremacy. *Nat Rev*
442 *Immunol* **2**, 675-687 (2002).
- 443 35. Seo, Y.J. & Hahm, B. Type I interferon modulates the battle of host immune system against
444 viruses. *Adv Appl Microbiol* **73**, 83-101 (2010).
- 445 36. McNab, F., Mayer-Barber, K., Sher, A., Wack, A. & O'Garra, A. Type I interferons in infectious
446 disease. *Nat Rev Immunol* **15**, 87-103 (2015).
- 447 37. Schneider, W.M., Chevillotte, M.D. & Rice, C.M. Interferon-Stimulated Genes: A Complex Web
448 of Host Defenses. *Annu Rev Immunol* **32**, 513-545 (2014).
- 449 38. Ahmed, M. et al. Ability of the matrix protein of vesicular stomatitis virus to suppress beta
450 interferon gene expression is genetically correlated with the inhibition of host RNA and protein
451 synthesis. *J Virol* **77**, 4646-4657 (2003).
- 452 39. Rieder, M. & Conzelmann, K.K. Rhabdovirus Evasion of the Interferon System. *J Interf Cytok*
453 *Res* **29**, 499-509 (2009).
- 454 40. Sherry, B. Rotavirus and Reovirus Modulation of the Interferon Response. *J Interf Cytok Res* **29**,
455 559-567 (2009).
- 456 41. Ng, C.S. et al. Encephalomyocarditis Virus Disrupts Stress Granules, the Critical Platform for
457 Triggering Antiviral Innate Immune Responses. *J Virol* **87**, 9511-9522 (2013).
- 458 42. Jensen, S. & Thomsen, A.R. Sensing of RNA viruses: a review of innate immune receptors
459 involved in recognizing RNA virus invasion. *J Virol* **86**, 2900-2910 (2012).
- 460 43. Goubau, D. et al. Antiviral immunity via RIG-I-mediated recognition of RNA bearing 5 '-
461 diphosphates. *Nature* **514**, 372-+ (2014).
- 462 44. Loo, Y.M. et al. Distinct RIG-I and MDA5 signaling by RNA viruses in innate immunity. *J Virol*
463 **82**, 335-345 (2008).
- 464 45. Honda, K. & Taniguchi, T. IRFs: master regulators of signalling by Toll-like receptors and
465 cytosolic pattern-recognition receptors. *Nat Rev Immunol* **6**, 644-658 (2006).
- 466 46. Ivashkiv, L.B. & Donlin, L.T. Regulation of type I interferon responses. *Nat Rev Immunol* **14**,
467 36-49 (2014).
- 468 47. Jowett, J.B. et al. The human immunodeficiency virus type 1 vpr gene arrests infected T cells in
469 the G2 + M phase of the cell cycle. *J Virol* **69**, 6304-6313 (1995).
- 470 48. Krauer, K.G. et al. The Epstein-Barr virus nuclear antigen-6 protein co-localizes with EBNA-3
471 and survival of motor neurons protein. *Virology* **318**, 280-294 (2004).

- 472 49. Darbinyan, A. et al. Evidence for dysregulation of cell cycle by human polyomavirus, JCV, late
473 auxiliary protein. *Oncogene* **21**, 5574-5581 (2002).
- 474 50. Everett, R.D., Earnshaw, W.C., Findlay, J. & Lomonte, P. Specific destruction of kinetochore
475 protein CENP-C and disruption of cell division by herpes simplex virus immediate-early protein
476 Vmw110. *EMBO J* **18**, 1526-1538 (1999).
- 477 51. Kramer, A., Green, J., Pollard, J., Jr. & Tugendreich, S. Causal analysis approaches in Ingenuity
478 Pathway Analysis. *Bioinformatics* **30**, 523-530 (2014).
- 479 52. Olive, C. Pattern recognition receptors: sentinels in innate immunity and targets of new vaccine
480 adjuvants. *Expert Rev Vaccines* **11**, 237-256 (2012).
- 481 53. Bohlson, S.S. Modulators of the innate immune response. *Curr Drug Targets* **9**, 101 (2008).
- 482 54. Mutwiri, G., Gerdts, V., Lopez, M. & Babiuk, L.A. Innate immunity and new adjuvants. *Rev Sci*
483 *Tech* **26**, 147-156 (2007).
- 484 55. Diamond, M.S. & Farzan, M. The broad-spectrum antiviral functions of IFIT and IFITM
485 proteins. *Nat Rev Immunol* **13**, 46-57 (2013).
- 486 56. Li, K. et al. IFITM proteins restrict viral membrane hemifusion. *PLoS Pathog* **9**, e1003124
487 (2013).
- 488 57. Pillai, P.S. et al. Mx1 reveals innate pathways to antiviral resistance and lethal influenza disease.
489 *Science* **352**, 463-466 (2016).
- 490 58. Verhelst, J., Hulpiau, P. & Saelens, X. Mx proteins: antiviral gatekeepers that restrain the
491 uninvited. *Microbiol Mol Biol Rev* **77**, 551-566 (2013).
- 492 59. Walsh, D., Mathews, M.B. & Mohr, I. Tinkering with translation: protein synthesis in virus-
493 infected cells. *Cold Spring Harb Perspect Biol* **5**, a012351 (2013).
- 494 60. Arpaia, N. & Barton, G.M. Toll-like receptors: key players in antiviral immunity. *Curr Opin*
495 *Virol* **1**, 447-454 (2011).
- 496 61. Kawai, T. & Akira, S. The roles of TLRs, RLRs and NLRs in pathogen recognition. *Int Immunol*
497 **21**, 317-337 (2009).
- 498 62. Thompson, A.J. & Locarnini, S.A. Toll-like receptors, RIG-I-like RNA helicases and the
499 antiviral innate immune response. *Immunol Cell Biol* **85**, 435-445 (2007).
- 500 63. Aaronson, D.S. & Horvath, C.M. A road map for those who don't know JAK-STAT. *Science*
501 **296**, 1653-1655 (2002).
- 502 64. Au-Yeung, N., Mandhana, R. & Horvath, C.M. Transcriptional regulation by STAT1 and STAT2
503 in the interferon JAK-STAT pathway. *JAKSTAT* **2**, e23931 (2013).
- 504 65. Li, H.S. & Watowich, S.S. Innate immune regulation by STAT-mediated transcriptional
505 mechanisms. *Immunol Rev* **261**, 84-101 (2014).
- 506 66. Hu, X. & Ivashkiv, L.B. Cross-regulation of signaling pathways by interferon-gamma:
507 implications for immune responses and autoimmune diseases. *Immunity* **31**, 539-550 (2009).

67. Fortier, M.E. et al. The viral mimic, polyinosinic:polycytidylic acid, induces fever in rats via an interleukin-1-dependent mechanism. *Am J Physiol Regul Integr Comp Physiol* **287**, R759-766 (2004).
68. Sharif-Askari, E. et al. Zinc finger protein Gfi1 controls the endotoxin-mediated Toll-like receptor inflammatory response by antagonizing NF-kappaB p65. *Mol Cell Biol* **30**, 3929-3942 (2010).
69. Tisserand, J. et al. Tripartite motif 24 (Trim24/Tif1alpha) tumor suppressor protein is a novel negative regulator of interferon (IFN)/signal transducers and activators of transcription (STAT) signaling pathway acting through retinoic acid receptor alpha (Raralpha) inhibition. *J Biol Chem* **286**, 33369-33379 (2011).
70. Gutierrez, J.M. & Lewis, N.E. Optimizing eukaryotic cell hosts for protein production through systems biotechnology and genome-scale modeling. *Biotechnol J* **10**, 939-949 (2015).
71. Kuo, C.C. et al. The emerging role of systems biology for engineering protein production in CHO cells. *Curr Opin Biotechnol* **51**, 64-69 (2018).
72. Richelle, A. & Lewis, N.E. Improvements in protein production in mammalian cells from targeted metabolic engineering. *Curr Opin Syst Biol* **6**, 1-6 (2017).
73. Taber, R., Alexander, V. & Wald, N., Jr. The selection of virus-resistant Chinese hamster ovary cells. *Cell* **8**, 529-533 (1976).
74. Haines, K.M., Vande Burgt, N.H., Francica, J.R., Kaletsky, R.L. & Bates, P. Chinese hamster ovary cell lines selected for resistance to ebolavirus glycoprotein mediated infection are defective for NPC1 expression. *Virology* **432**, 20-28 (2012).
75. FDA Guidance for industry: Q5A viral safety evaluation of biotechnology products derived from cell lines of human or animal origin. (1998).
76. FDA Guidance for industry: Characterization and qualification of cell substrates and other biological starting materials used in the production of viral vaccines for the prevention and treatment of infectious diseases. (2006).

536 Tables

537 **Table 1. Study prototype viruses and multiplicity of infection (MOI) on CHO-K1 cells.**

538

Virus	Virus family	Genomic nucleic acid nature	Referenced CHO cell culture infection	MOI
Vesicular stomatitis virus (VSV)	Rabdoviridae	ss (-) RNA	Potts, 2008	0.003
Encephalomyocarditis virus (EMCV)	Picornaviridae	ss (+) RNA	Potts, 2008	0.007
Reovirus 3 (Reo-3)	Reoviridae	ds RNA	Wisher, 2005; Rabenau 1993	0.0013

539

540

541

542

543

544 **Table 2A. The downstream effects of the upstream regulators from the comparison of m vs. p.**

Virus	Consistency score ^a	Total nodes (TF, TG, BP)	Transcription factors (TF) ^b	Target gene (TG) ^c	Biological Process (BP) ^d	Relations ^e
30h	5.82	21 (5, 13, 3)	STAT1, IRF3, IRF5, IRF7, NFATC2	CASP1, CXCL10, DDX58, EIF2AK2, IFIH1, IL15, ISG15, Mx1/Mx2, OASL2, PELI1, PML, SOCS1, TNFSF10	Inhibit Replication of virus. Activate Activation of phagocytes; Apoptosis of antigen presenting cells.	6/15 (40%)
54 h	22.47	48 (7.29.12)	STAT1, IRF3, IRF5, IRF7, NFATC2, TRIM24, NCOA2	BST2, C3, CASP1, CXCL10, DDX58, EGR2, EIF2AK2, GBP2, IFIH1, IFIT1B, IFIT2, IFITM3 (IITMP3), Igtp, IL15, ISG15, Mx1/Mx2, MYC, OASL2, PML, PSMB10, PSMB8, PSME2, PTGS2, SPP1, STAT2, TAP1, TLR3, TNFSF10, TRAFD1	Inhibit Replication of virus; Infection by RNA virus; Infection of central nervous system. Activate Antiviral response; Clearance of virus; Immune response of antigen presenting cells; Immune response of phagocytes; Cytotoxicity of leukocytes; Function of leukocytes; Infiltration by T lymphocytes; Quantity of MHC Class I of cell surface; Cell death of myeloid cells.	21/84 (25%)
78 h	27.80	30 (8, 14, 8)	STAT1, IRF5, NFATC2, NR3C1, PPARD, ZBTB16, CDKN2A, EBF1	C3, CCL2, CCL7, CD36, CXCL10, CXCL9, DDX58, EIF2AK2, ISG15, MYC, THBS1, TLR3, TNFSF10, VEGFA	Activate Activation of macrophages; Apoptosis of myeloid cells; Cell movement of T lymphocytes; Cellular infiltration by leukocytes; Damage of lung; Recruitment of leukocytes; Response of myeloid cells; Response of phagocytes.	11/64 (17%)
78 h	7.56	12 (2, 7, 3)	CDKN2A, ZBTB16	C3, CCL2, CCL7, CXCL10, CXCL9, MYC, VEGFA	Activate Cell movement of T lymphocytes; Recruitment of leukocytes; Survival of organism.	1/6 (17%)

545

546 **Table 2B. The downstream effects of the upstream regulators from the comparison of Vm vs. Vp.**

Virus	Consistency score	Total nodes (TF, TG, BP) ^{*a}	Transcription factors (TF) ^{*b}	Target genes (TG) ^{*c}	Biological Process (BP) ^{*d}	Relationships ^{*e}
VSV	8.00	22 (4, 15, 3)	STAT1 , IRF3, IRF5, IRF7	CXCL10, DDX58, EIF2AK2, IFIH1, IL15, ISG15, JUN, Mx1/Mx2, OASL2, PSMB10, PSMB8, PSMB9, SOCS1, TAP1, TNFSF10	Inhibit Replication of virus; Quantity of lesion. Activate Quantity of CD8+ T lymphocyte.	2/12 (17%)
EMCV	12.16	29 (6, 19, 4)	STAT1 , IRF3, IRF5, IRF7, TRIM24, ATF4	BST2, CXCL10, DDX58, EIF2AK2, EIF4EBP1, IFIH1, IL15, ISG15, Mx1/Mx2, OASL2, PSMB10, PSMB8, PSMB9, SLC1A5, SLC3A2, SLC6A9, SLC7A5, TAP1, TNFSF10	Inhibit Replication of virus; Transport of amino acids. Activate Quantity of CD8+ T lymphocyte; Quantity of MHC Class I on cell surface.	3/24 (13%)
EMCV	7.91	18 (2, 10, 6)	CCND1, SMAD4	AREG, CCND2, EREG, GJA1, HSPA8, ITGAV, NFKBIA, PTGS2, SOX4, SPP1	Inhibit Arthritis; Cell cycle progression; Cell viability; Growth of ovarian follicle; Proliferation of cells. Activate Edema.	7/12 (58%)
EMCV	6.96	19 (2, 10, 7)	MKL1, VDR	CAMP, CCL2, HLA-A, ICAM1, IL6, MMP9, PTGS2, RELB, SPP1, TNC	Inhibit Cancer; Quantity of interleukin; Rheumatic Disease; Development of body trunk. Activate Cell death of connective tissue cells; Nephritis; Organismal death.	7/14 (50%)
Reo-3	5.61	21 (4, 14, 3)	GF11, NR1H3, NRIP1, PPARG	ACACB, CAV1, CD36, CSF3, ETS1, ID2, IL6, LDLR, LPL, NFKBIA, PDK2, PDK4, PPARA, SLC2A1	Inhibit Oxidation of carbohydrate; Production of leukocytes; Quantity of vldl triglyceride in blood.	1/12 (8%)

547 ^{*a} Consistency score is to measure the consistency of a predicted network by IPA with the literature evidences.

548 ^{*b,c} The upstream regulators (STAT1 is highlighted in bold face) and the antiviral relating genes.

549 ^{*d} The biological functions known to associated with the regulatory networks annotated by the IPA.

550 ^{*e} The number of identified relationships and the total relationships that represent the known regulatory
551 relationships between regulators and functions supported by literatures annotated by the IPA.

552 List of Figures and Legends

553 **Figure 1. RNA viruses induce cytopathic effects on CHO-K1 cells.** (A) Cytopathic effect of the three
554 RNA viruses on CHO cells upon 30h (VSV), 54h (EMCV) or 78h (Reo-3) of infection. Fold change in
555 IFN β (B) and Mx1 (C) gene expressions in CHO cells infected with the three RNA viruses compared to
556 uninfected cells at the same time points. (D) Several pathways and processes were enriched for
557 differentially expressed genes following viral infection (m vs. Vm). (E) Top activated (red) or repressed
558 (blue) upstream regulators following virus infection.

559 **Figure 2. Innate immunity genes in CHO cells are activated by poly I:C.** (A) IFN-stimulated
560 transcription was increased in cells treated with poly I:C /LyoVec for 24h, but not with other TLR ligands
561 engaging TLR9, TLR4 or TLR7/8. (B) Poly I:C triggered STAT1 phosphorylation in a dose dependent
562 manner, and (C) the levels of STAT2 phosphorylation and Mx1 protein expression were comparable to
563 those triggered by IFN α 2c. (D) Several pathways and processes were enriched for differentially
564 expressed genes following poly I:C treatment (m vs. p). (E) Top upstream regulators that are activated
565 (red) or repressed (blue) following poly I:C treatment.

566 **Figure 3. Poly I:C pre-treatment prevents virus infection of VCV, EMCV, and Reo-3.** (A-C) Cell
567 morphology (left panels) and cytopathic effect measured by crystal violet staining (right panels) of virus-
568 infected CHO cells; (D) The enriched down-stream pathways under condition of Vm vs. Vp using RNA-
569 Seq data. (E) The top 35 upstream regulators that are activated or repressed by poly I:C pre-treatment.
570 A full list of the activated or repressed upstream regulators is shown in the Table S5.

571 **Figure 4. A STAT1-dependent regulatory network controls viral resistance (VSV and EMCV) in**
572 **CHO cells.** A STAT1-dependent regulatory network induced by the pre-treatment of poly I:C leads to
573 the inhibition of VSV (A) and EMCV (B) replication in CHO cells, based on the comparison of Vm and

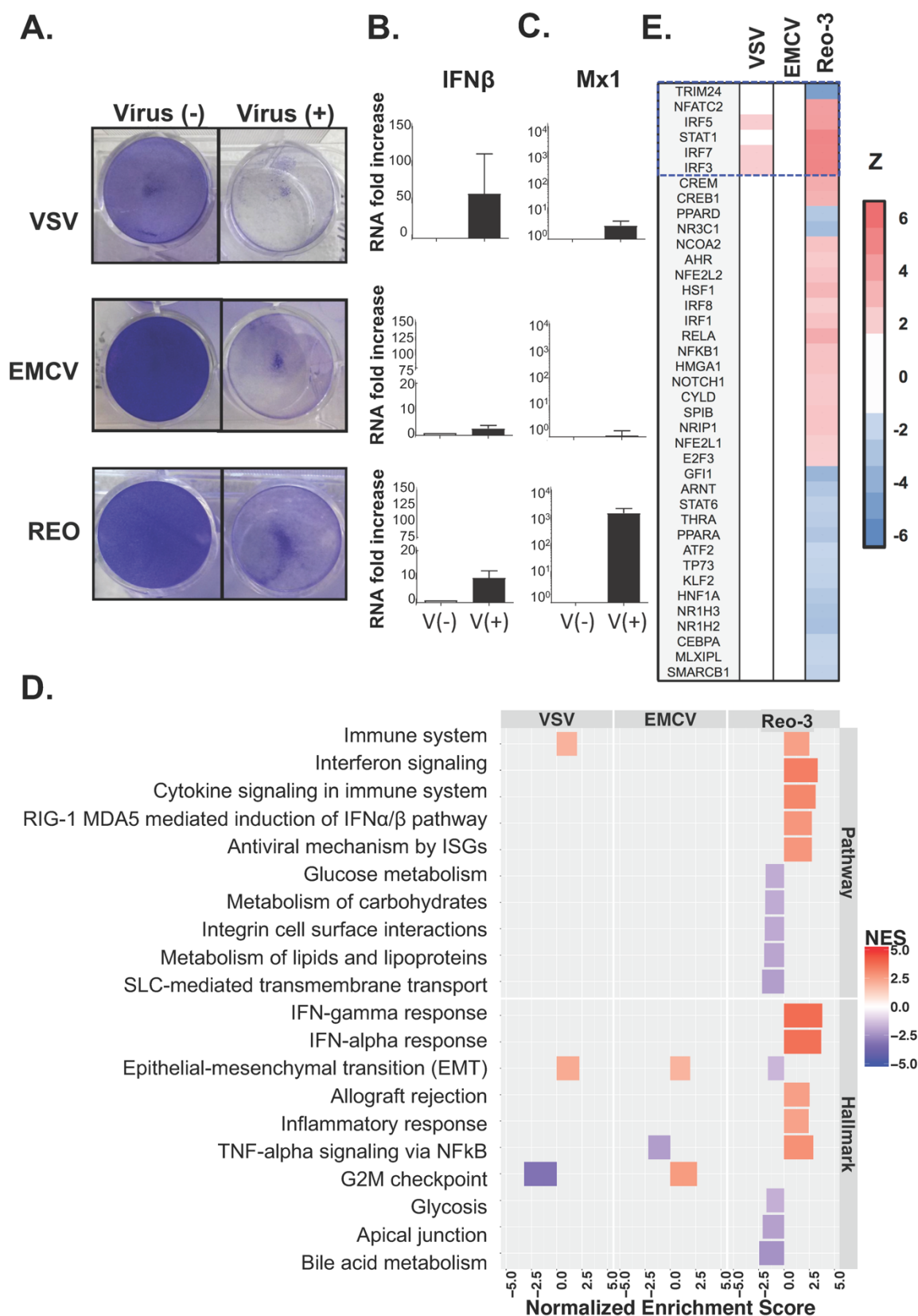
574 Vp RNA-Seq. The colors denote the states inferred from the RNA-Seq data. For example, the blue color
575 of TRIM24 means that TRIM24 activity is suppressed, based on the differential expression of genes that
576 are regulated by TRIM24.

577 **Figure 5. Identification of regulators of STAT1 as candidates for engineering the antiviral**
578 **response.** Schematic of the regulators of STAT1, which may be candidates for engineering and
579 improving virus resistance in CHO cells.

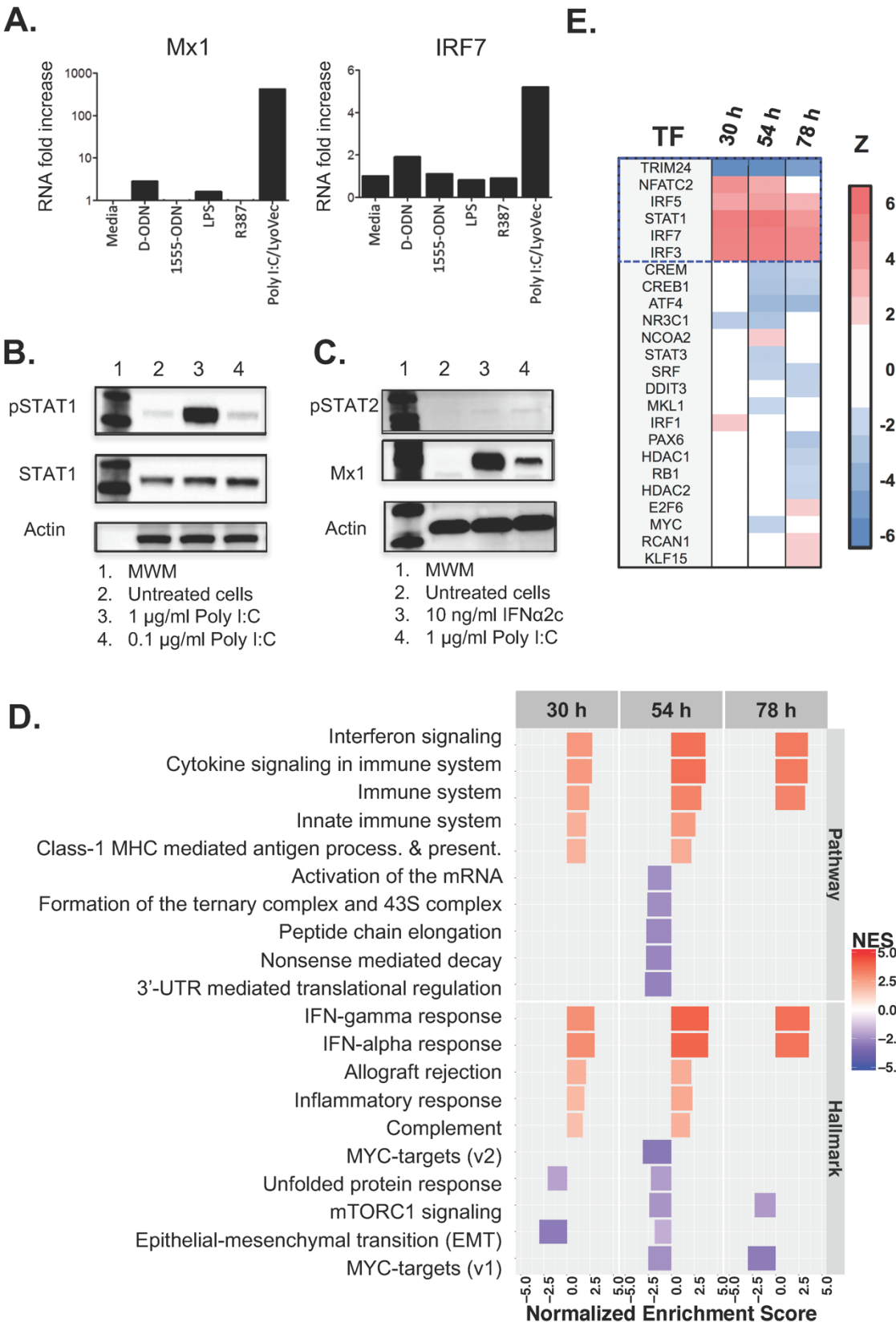
580 **Figure 6. Viral resistance of the Gfi1 and/or Trim24 KO engineered CHO cells.** Gfi1 and Trim24
581 were knocked out and tested for resistance to EMCV and Reo-3 virus infection compared to the control
582 (susceptible) cells. Cell density and viability was followed up for one week post infection (p.i.) for Gfi1
583 single knockout cells (A), Trim24 single knockout cells (B) and Gfi1 and Trim24 double knockout cells
584 (C). Data shown is from three (EMCV) and two (Reo-3) independent virus infection experiments.
585 Susceptible CHO cell lines were used as positive controls for EMCV and Reo-3 virus infections during
586 the first seven days (Figure S10). In some experiments, resistant cultures were passaged and followed
587 up for an additional week (Figure S11).

588
589

Figure 1. Virus infection effects on CHO cells

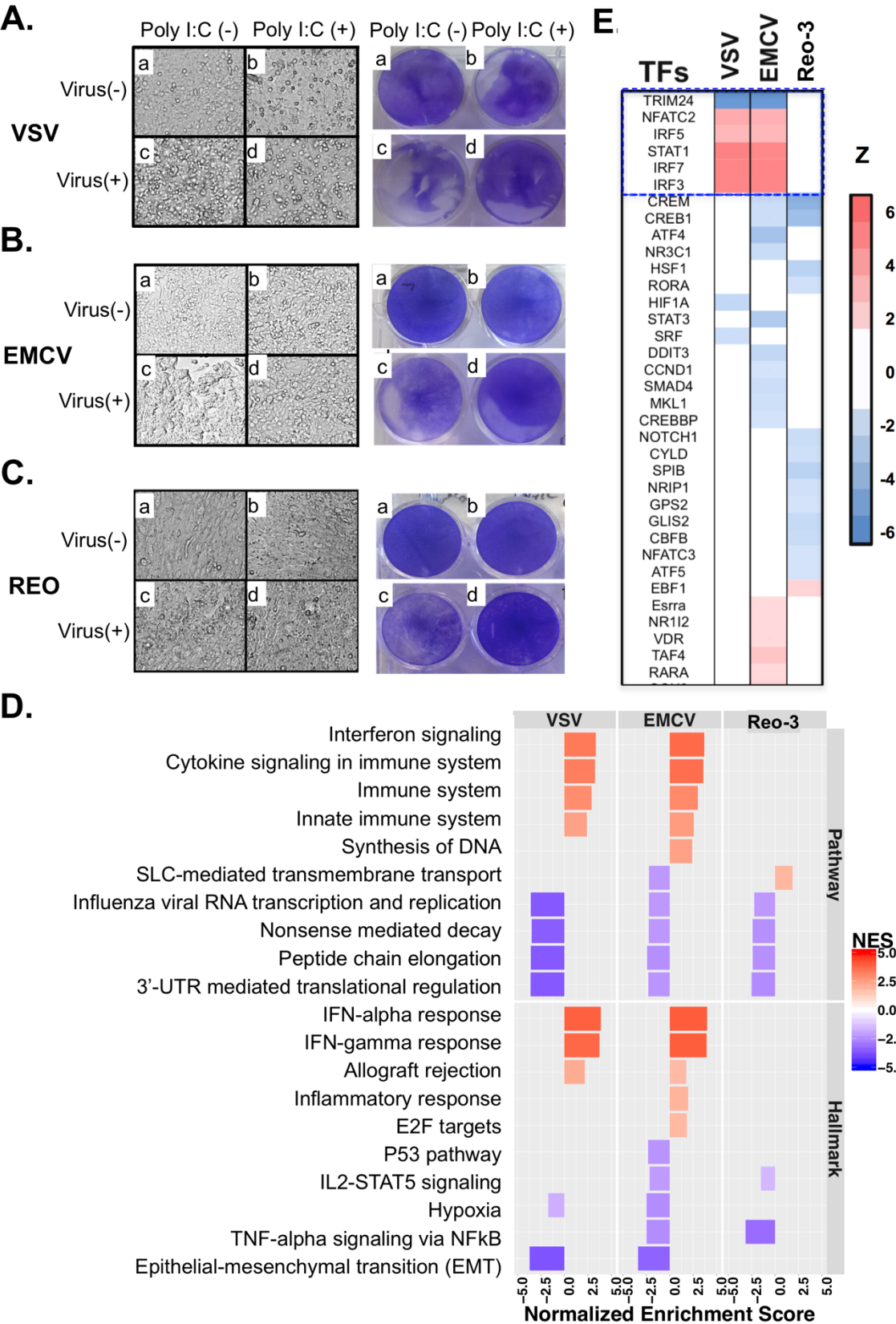


592 **Figure 2. Innate immunity genes in CHO cells are activated mainly by poly I:C**



593
594

595 **Figure 3. Poly I:C pretreatment inhibits virus infection of VCV, EMCV, and Reo-3.**

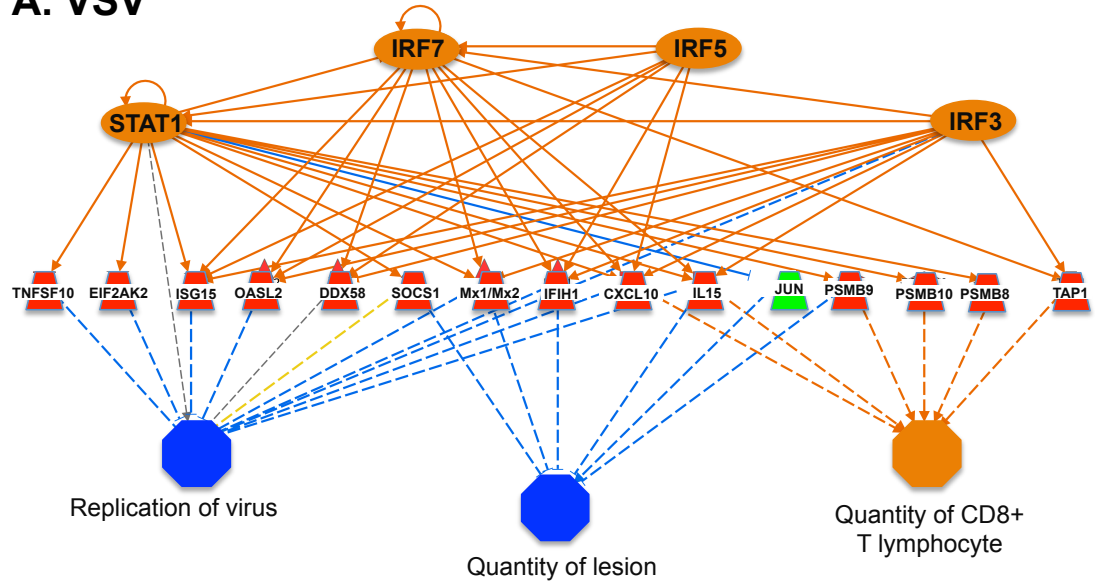


597 **Figure 4. A STAT1-dependent regulatory network controls viral resistance (VSV**
598 **and EMCV) in CHO cells.**

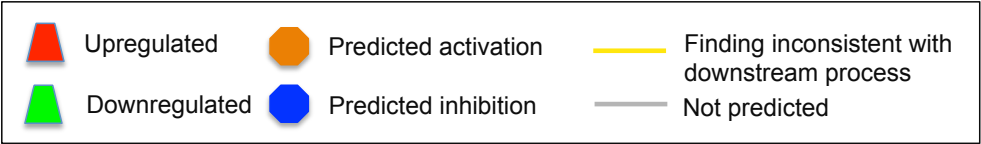
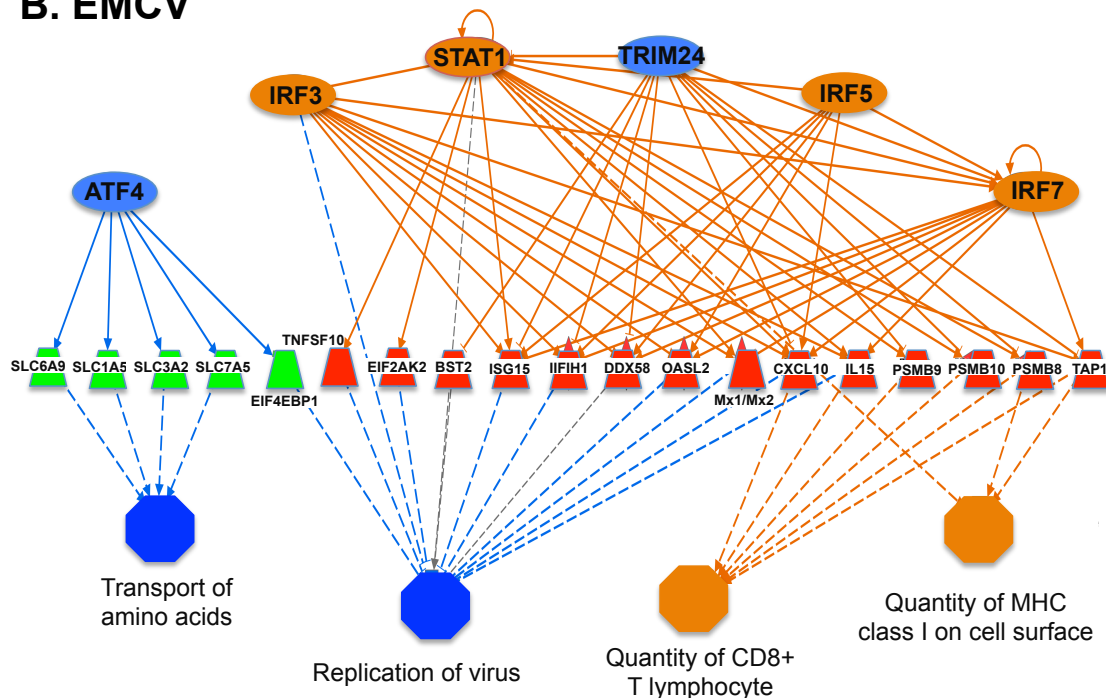
599

600

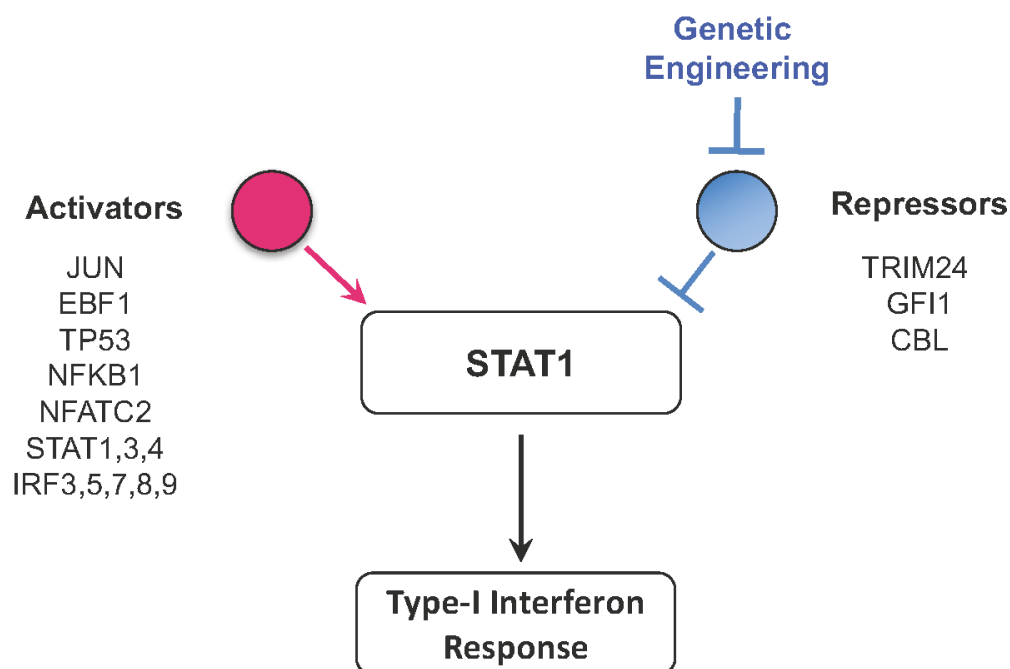
A. VSV



B. EMCV



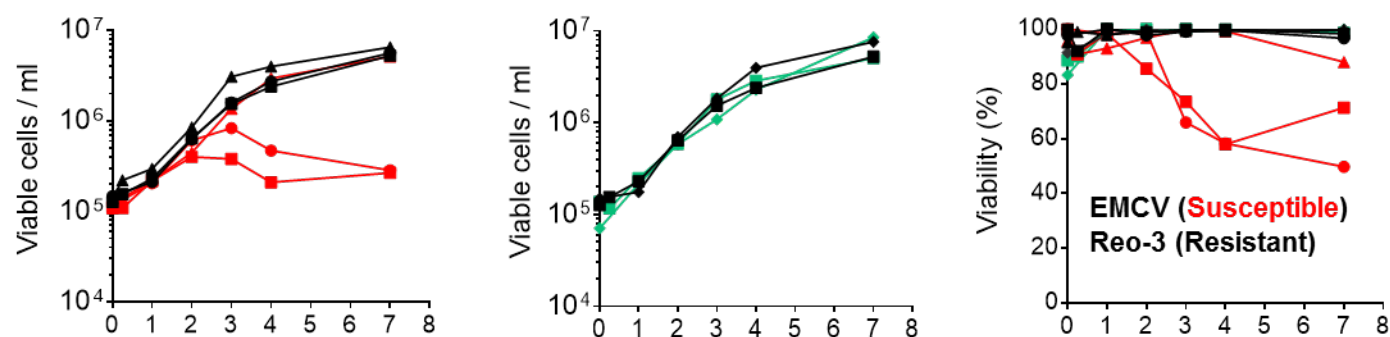
601 **Figure 5. Identification of regulators of STAT1 as candidates for engineering the**
 602 **antiviral response.**



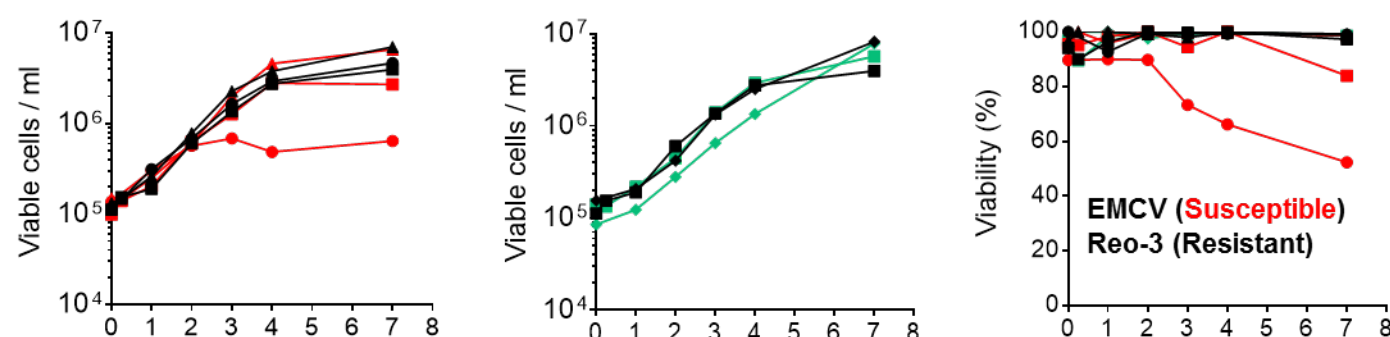
603
 604

Figure 6. Viral resistance of the Gfi1 and/or Trim24 engineered CHO-S cells.

A. Gfi1 KO



B. Trim24 KO



C. Gfi1+Trim24 KO

